J. Fluid Mech. (1970), *vol.* 44, *part* 4, *pp.* 741–765
Printed in Great Britain

An experimental study of non-linear interaction of velocity fluctuations in the transition region of a two-dimensional wake

By HIROSHI SATO

Institute of Space and Aeronautical Science, University of Tokyo, Japan

(Received 10 February 1970)

As an extension of our previous work (Sato & Kuriki 1961), an experimental study was made on the laminar-turbulent transition of a two-dimensional wake, with emphasis on the non-linear interaction of velocity fluctuations. In the natural transition, a sinusoidal velocity fluctuation first appears as a result of the selective amplification of irregular disturbances. When the amplitude of the fluctuation becomes large, a non-linear interaction takes place: higher harmonics of the sinusoidal fluctuation and a slow, irregular fluctuation are generated. The transition into turbulence is gradual, and there are no abrupt 'breakdowns'.

When a sound with two frequencies (f_1 and f_2) is introduced into the wake, two velocity fluctuations are induced. They are amplified independently when amplitudes are small. If amplitudes exceed certain values, a mutual interaction takes place, and the growth of each component is suppressed by the presence of the other. At the same time, fluctuations with frequencies of f_1-f_2, $2(f_1-f_2)$ ... and f_1+f_2, $2(f_1+f_2)$ ... are produced. The behaviour of the slow, irregular fluctuation in the natural transition closely resembles that of the f_1-f_2 component. They seem to be produced by the same mechanism.

In the transition region of the wake, a small variation in the amplitude of velocity fluctuation is enhanced by the suppression effect, and a small irregularity in the frequency is amplified by the generation of the f_1-f_2 component. These are two elementary processes of randomization of regular fluctuations, which lead to the development of turbulence.

1. Introduction

In recent years, extensive studies have been made of the laminar-turbulent transition of free flows such as jets, wakes and separated layers. Results of the linear stability theory for those flows show good agreements with experimental observations, when the amplitude of the fluctuation is small. When the amplitude exceeds a certain value, the linear theory is no longer valid. The basic flow is distorted by the Reynolds stress and the distortion, in turn, modifies the growth of the fluctuation. Therefore, both mean flow and the fluctuation must be considered simultaneously. Theoretical investigations on this non-linear problem have been made for the free flow (Benney 1961; Kelly 1968), but details of

the effect of the non-linear interaction on the transition process are not yet clear.

Experimental investigations indicate that the transition process of the free flow is very different from that of the boundary layer along a plate. The transition of the boundary layer is characterized by the occurrence of abrupt 'breakdowns', while in the free flow the transition is accomplished by a gradual change. Among free flows there are differences in the transition process. For instance, in the asymmetrical separated layer, Sato (1959) and Browand (1966) observed subharmonics of the predominant velocity fluctuation, but in the symmetrical wake no such subharmonics have been found (Sato & Kuriki 1961). These facts indicate that more experimental work is still needed for a full understanding of the transition process.

An important phase in the transition is concerned with the role of the initial disturbance. The fully-developed turbulent flow is in an equilibrium state and the structure of the turbulent field should be independent of initial conditions. On the contrary, the whole transition process strongly depends on the initial disturbance. The 'natural' transition is initiated by small natural disturbances in the flow. When an artificial disturbance is introduced, the transition takes place in a different manner. If the artificial disturbance is regular, we observe the change of a regular fluctuation into random turbulence. Although this randomization is an essential feature of the transition, it has not been studied extensively. Discussions on the wave form of the fluctuation have been mostly qualitative. From a theoretical viewpoint, existing non-linear stability theories are deterministic in nature. They are concerned only with regular fluctuations. The theory of turbulence, on the other hand, assumes a full randomness. There is no theory connecting these two states.

The purpose of the present investigation is to clarify the non-linear interaction and the randomization process experimentally. Detailed measurements were made on mean and fluctuating velocities in a two-dimensional wake with two different initial conditions. One is the natural transition without artificial disturbances. The other is the transition in the presence of sound from a loudspeaker. The sound induces a small-amplitude velocity fluctuation in the wake. The fluctuation is amplified in the linear region, if the frequency is properly chosen. Using a sound composed of two frequencies, the non-linear interaction of two velocity fluctuations was investigated. Randomizations of regular velocity fluctuations were observed by spectral analysis. Only a portion of the results is presented here. A more complete description of the experimental data will be found in Sato & Onda (1970).

2. Experimental arrangement

The experiment was conducted in the no. 2 Low-Turbulence Wind-Tunnel at the Institute of Space and Aeronautical Science. The tunnel is of straight blow-out type, and has a closed test-section of 60 cm by 60 cm cross-section and 3 m length. The cross-section of the settling chamber is 2·4 m by 2·4 m, and the contraction ratio is 16. The residual longitudinal turbulence level, $\sqrt{u^2}/U_0$, is about

0·04 % at a wind-speed of 10 m/sec. The streamwise distribution of the static pressure was made uniform within 1 % of the dynamic pressure, by adjusting side walls. One of the side walls has slits in horizontal and vertical directions. A static-pressure probe or a hot-wire anemometer mounted on a three-dimensional traversing mechanism was inserted into the test-section through those slits.

For producing a two-dimensional wake, a flat plate of 3 mm thickness and 30 cm length was set in the test-section parallel to the flow as shown in figure 1. The leading edge of the plate forms a half of 10:1 ellipse and the rear part of the plate is tapered off symmetrically with a gradient of 1:100 to form a thin trailing edge. In Sato & Kuriki (1961), the trailing edge was made as thin as possible and it was slightly wavy. In the present experiment, the trailing edge was made straight with the expense of thinness. The trailing edge is about 0·2 mm thick. A symmetrical disturbance-free wake was produced behind the plate. The co-ordinate system has an origin at the centre of the trailing edge. The X-axis is in the flow direction, the Y-axis perpendicular to the plate, and the Z-axis is parallel to the trailing edge.

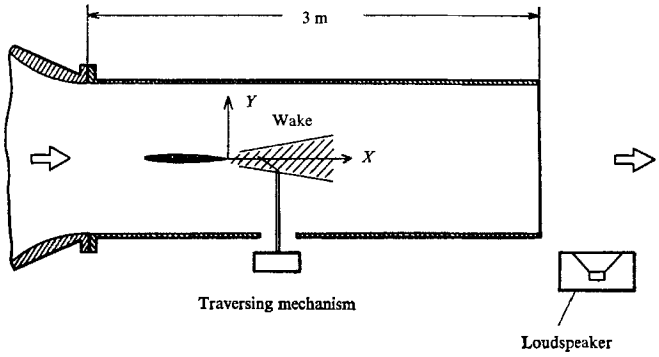

FIGURE 1. Layout of test-section. Cross-section 60 × 60 cm, length of plate 30 cm, thickness 3 mm.

Two turbulent wedges expand in the boundary layer of the plate, starting from intersections of the leading edge of the plate and ceiling and floor of the test-section. The expansion angle of this 'transverse contamination' was found to be about 11 degrees. The region $|Z| < 8$ cm is contamination-free at $X = 800$ mm, which is the downstream limit of the range of the present experiment.

A 10 W loudspeaker was placed at the end of the test-section. A signal from an audio frequency oscillator was fed to the loudspeaker for introducing sound into the wake. Two oscillators were used for producing sound with two frequencies. Changes in the location of the loudspeaker and the direction of the sound show no substantial difference in experimental results.

The pressure in the wake was measured by a small static pressure probe. Measurements of mean and fluctuating velocities were made by constant temperature hot-wire anemometers. The velocity component in the flow direction was measured by a single hot-wire, and components in Y- and Z-directions were measured by X-type wires. As the hot-wire a tungsten wire of 3·8 μ diameter, and about 1 mm length was used. Amplifiers for hot-wires were all d.c. coupled and

the output from the hot-wire was linearized. A band-pass filter was used for the spectral analysis. The position of the hot-wire was transformed into an electric signal and recorded on an $X-Y$ recorder together with the hot-wire output. The error in the absolute measurement of $\overline{u^2}$ is probably not more than 10 %. Errors are mainly due to the slight non-linearity and temporal change of the calibration curve of the hot-wire. Relative values are more accurate. In the measurement of v- and w-fluctuations, errors due to mismatching and misalignment of two wires are added. Besides those, an X-wire for measuring v-fluctuations has a length of about 0·7 mm in the Y-direction. Therefore, the output is an averaged value in the Y-direction. The maximum error in the absolute values of $\overline{v^2}$ may be as high as 20 %. The accuracy for $\overline{w^2}$ may be a little better. But, when $\overline{w^2}$ is very small compared with $\overline{u^2}$ or $\overline{v^2}$, the error due to the mismatching and misalignment of X-wires is very large, and it always leads to larger values of $\overline{w^2}$.

All measurements were made at a fixed free-stream velocity, 10 m/sec. The thickness of the boundary layer at the trailing edge with this wind-speed was about 2 mm. The Reynolds number based on the thickness was 1500.

The reproducibility of the flow field is not good in the natural transition, because we cannot control the residual disturbance in the wind-tunnel. The disturbance may change from day to day. Measured absolute intensity and frequency of fluctuations in natural transition are slightly different for different runs, while relative values are maintained almost unchanged. When the sound is introduced, the reproducibility is much improved. We noticed, however, that sound of the same intensity did not result in a velocity fluctuation of the same amplitude on different days. Therefore, in order to assure the same effect of sound, we adjusted the intensity of sound, and made the amplitude of the induced velocity fluctuation the same for each run.

3. Natural transition

The boundary layer along the plate is laminar, and the velocity distribution is of Blasius type. The velocity distribution in the wake is shown in figure 2. The mean velocity U in the figure is normalized by the free-stream velocity U_0. The non-dimensional velocity on the centre-line increases from zero at the trailing edge to 0·85 at $X = 100$ mm. It decreases to 0·78 at $X = 150$ mm, and then increases downstream again. Distributions at various X-stations are almost similar except at $X = 150$ mm, where U/U_0 exceeds unity at around $Y = \pm 6$ mm. In the wake of a bluff body, this overshoot is not strange, because the flow is accelerated at both shoulders of the body. But, for a thin flat plate, such an acceleration does not take place, and the large value of U at the edge of wake is produced by the non-linear interaction between the mean velocity and velocity fluctuations. Streamwise variations of the non-dimensional central velocity U_c/U_0, and the half-value breadth b, are illustrated in figure 3. The sharp increase in b at $X = 35$ mm indicates the start of the non-linear interaction region. Both U_c/U_0 and b reach maximum at around $X = 80$ mm, and then decrease. At around $X = 200$ mm both become minima and gradually increase again. A part of these results has been reported in Sato & Kuriki (1961). These complicated streamwise

variations of U_c/U_0 and b might be connected to the energy exchange between the mean motion and fluctuations. A detailed discussion of this point is to be found in § 5.

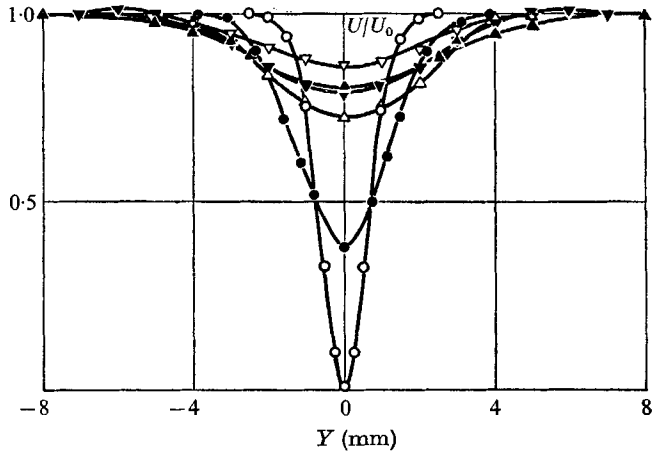

FIGURE 2. Mean velocity distributions. Natural transition. Free-stream velocity, $U_0 = 10$ m/sec. X (mm): ○, 1; ●, 40; △, 60; ▽, 100; ▼, 150; ▲, 400.

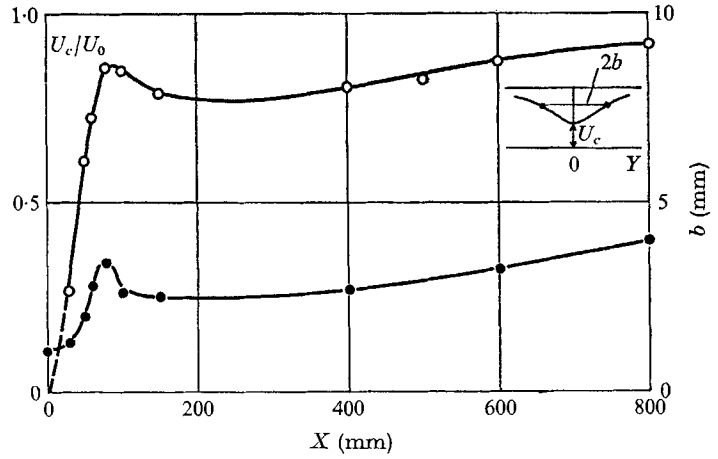

FIGURE 3. Streamwise variations of velocity on the centre-line U_c, ○ and half-value-breadth b, ●. Natural transition.

Lateral mean velocity components, V and W are very small. The maximum value of V in the whole transition region is around 3 % of U_0, and W is less than that. The static pressure in the laminar portion of the wake is the same as that of the free stream. In the non-linear region, the pressure is negative. The maximum negative pressure occurs on the centre-line at $X = 80$ mm, the value being about 3 % of the dynamic pressure ($\frac{1}{2}\rho U_0^2$). This negative pressure is also relevant to the non-linear interactions.

Near the trailing edge of the plate there are no velocity fluctuations. A periodic small amplitude velocity fluctuation first appears at $X = 20$ mm. The fluctuation

grows exponentially in the flow direction as described in Sato & Kuriki (1961). The predominant frequency of the natural fluctuation in the present experimental condition is about 630 Hz. The growth rate of the fluctuation with this frequency is almost maximum according to the linear stability theory.

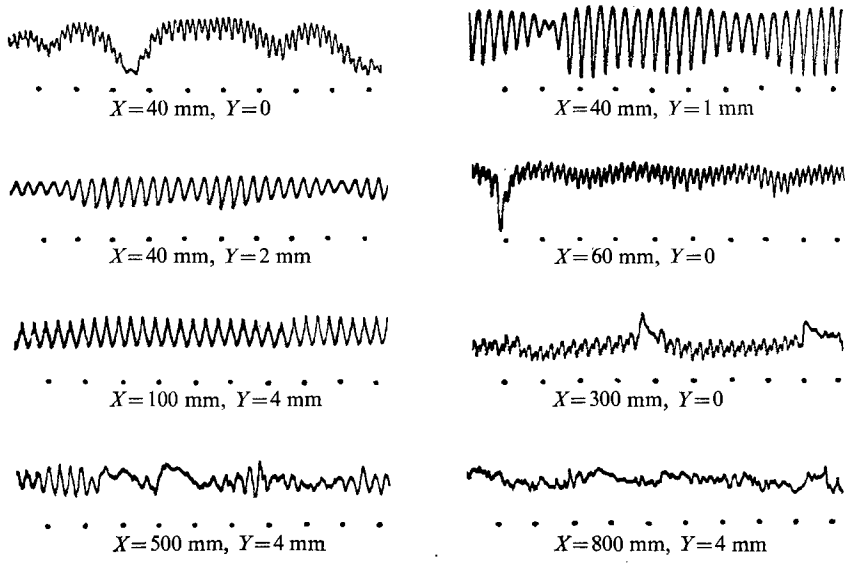

FIGURE 4. Wave-forms of u-fluctuations. Natural transition. Velocity increases upward. Time from left to right and time interval between dots is 5 msec.

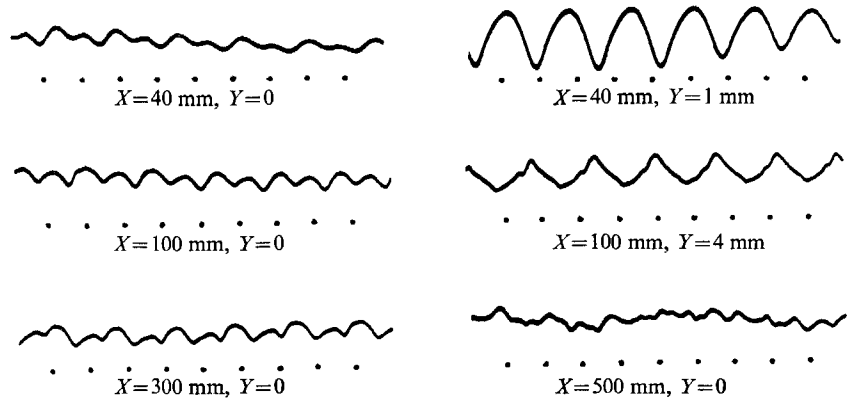

FIGURE 5. Wave-forms of u-fluctuations. Natural transition. Time interval between dots is 1 msec.

Wave-forms of u-fluctuations are reproduced in figures 4 and 5 with two different sweep speeds. Figure 4, with slower sweep speed, shows details of low frequency fluctuations. Wave-forms at $Y \neq 0$ are regular and periodic at small X (for example, $X = 40$ mm, $Y = 2$ mm and $X = 100$ mm, $Y = 4$ mm). On the other hand, fluctuations on the centre-line are composed of second harmonics (1260 Hz) and a slow, irregular component (for example, $X = 40$ mm, $Y = 0$

and $X = 60\,\text{mm}$, $Y = 0$). At $X = 500\,\text{mm}$, $Y = 4\,\text{mm}$, both periodic and irregular components are present. A turbulent pattern is established at $X = 800\,\text{mm}$. The change of the wave-form in the flow direction is gradual. No 'bursts' or 'breakdowns' are found. Details of high-frequency components are shown in figure 5 with higher sweep speed. The 1260 Hz-fluctuation is observed on the centre-line at X-stations from 40 mm to 300 mm. At $Y \neq 0$ the fundamental component is predominant. At $X = 40\,\text{mm}$, $Y = 1\,\text{mm}$ the wave-form is almost sinusoidal, whereas the wave-form at $X = 100\,\text{mm}$, $Y = 4\,\text{mm}$ is very much deformed. This change implies that several higher harmonics are generated between these two X-stations. The process of natural transition is characterized by the production of irregular low frequency components near the centre-line and the systematic generation of higher harmonics.

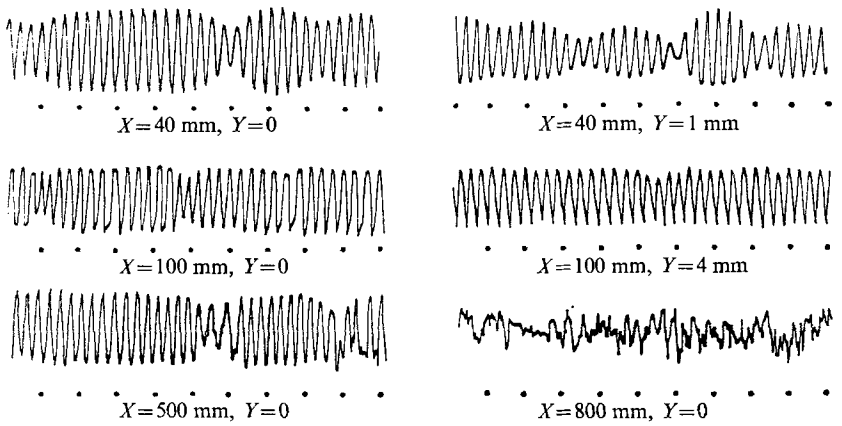

FIGURE 6. Wave-forms of v-fluctuations. Time interval between dots is 5 msec. Natural transition.

Wave-forms of v-fluctuations are shown in figure 6. They are different from those of u-fluctuations in many respects. First of all, wave-forms on the centre-line are composed mostly of the regular fundamental component. Second harmonics as well as the slow, irregular fluctuation are weak. Wave-forms at $Y = 0$ and $Y \neq 0$ do not show much difference. They are all distorted in various fashions but the fundamental component exists at all points until $X = 500\,\text{mm}$. Wave-forms at large X are more regular than those of u-fluctuations (for example, $X = 500\,\text{mm}$ and $Y = 0$). At $X = 800\,\text{mm}$, the wave-form is irregular and turbulent.

Distributions of $\overline{u^2}$, $\overline{v^2}$ and $\overline{uv}$ are shown in figures 7 and 8 at two X-stations in the non-linear region. They are non-dimensionalized by the free-stream velocity U_0. At $X = 40\,\text{mm}$ (figure 7) the distribution of $\overline{u^2}/U_0^2$ has a minimum on the centre-line and two peaks at $Y = \pm 1\,\text{mm}$, maximum values being about 1×10^{-2}. The distribution of $\overline{v^2}/U_0^2$ shows a maximum on the centre-line, the value being $0{\cdot}5 \times 10^{-2}$. These two distributions are close to distributions of small-amplitude fluctuations calculated by the linear theory. The non-dimensional cross correlation $\overline{uv}/U_0^2$ is zero on the centre-line and is negative at $Y > 0$. The location of

the maximum of uv almost coincides with that of the maximum of the shear $\partial U/\partial Y$. At $X = 100$ mm (figure 8) $\overline{u^2}/U_0^2$ has a flat distribution between $Y = 4$ mm and -4 mm and the maximum value is only $\frac{1}{4}$ of that at $X = 40$ mm. On the other hand, the maximum value of $\overline{v^2}/U_0^2$ increases between two X-stations by about

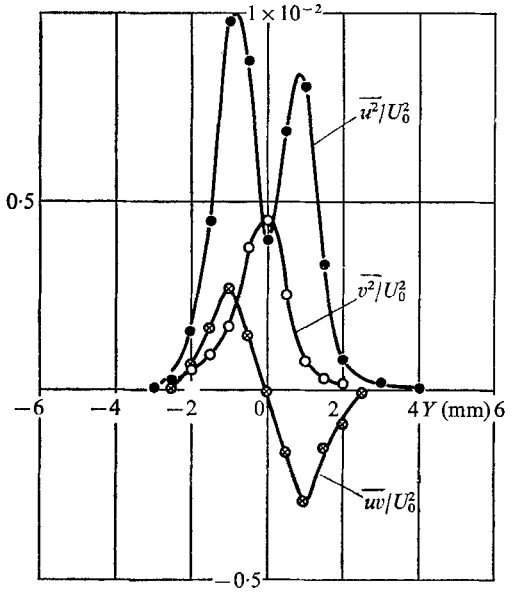

FIGURE 7. Distributions: ●, $\overline{u^2}/U_0^2$; ○, $\overline{v^2}/U_0^2$; ⊗, $\overline{uv}/U_0^2$. $X = 40$ mm. Natural transition.

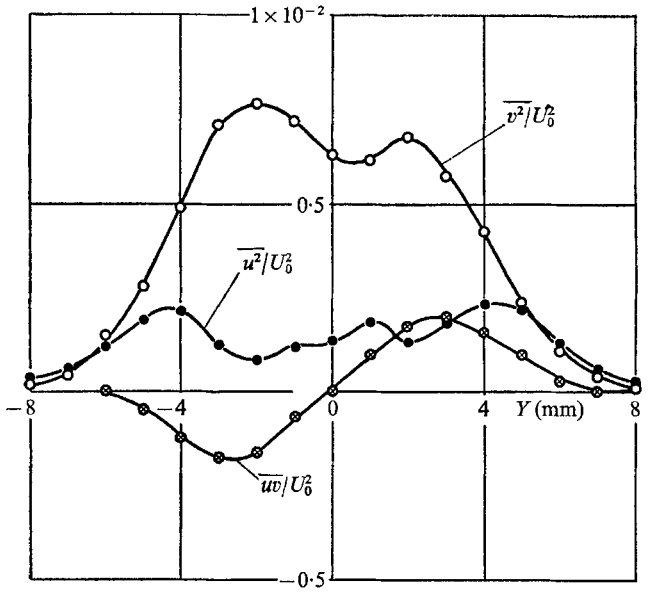

FIGURE 8. Distributions: ●, $\overline{u^2}/U_0^2$; ○, $\overline{v^2}/U_0^2$; ⊗, $\overline{uv}/U_0^2$. $X = 100$ mm. Natural transition.

1·5 times. This remarkable decrease of $\overline{u^2}$ is a result of the energy exchange as will be shown later. The sign of $\overline{uv}$ at $X = 100$ mm is reversed, namely, $\overline{uv}$ is positive at $Y > 0$. Experimental results at various X-stations indicate that the negative $\overline{uv}$ at $Y > 0$ occurs for positive values of $\partial U_c/\partial X$, and negative $\partial U_c/\partial X$ corresponds to the positive $\overline{uv}$ at $Y > 0$. At the X-station where $\partial U_c/\partial X$ is zero, $\overline{uv}$ is almost zero.

The overall mean square values, $\overline{u^2}$ and $\overline{v^2}$, are sums of many spectral components. Distributions of various spectral components are not the same. The u-fluctuation of the fundamental component (630 Hz) has a minimum at $Y = 0$, and two off-centre maxima at all X-stations from 20 mm to 150 mm, as shown in

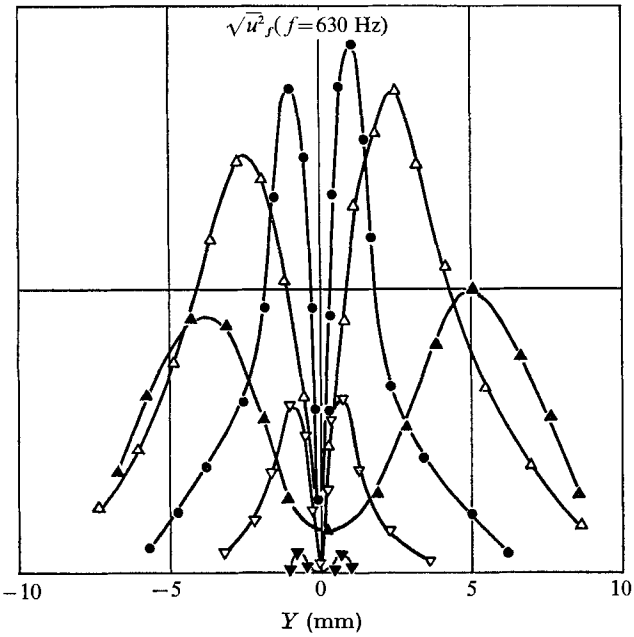

FIGURE 9. Distributions of fundamental (630 Hz) component. Natural transition. The ordinate scale is arbitrary. X (mm): ▽, 20; ▼, 30; ●, 40; △, 60; ▲, 150.

figure 9. The phase of the u-fluctuation of the fundamental component is anti-symmetrical with respect to the centre-line, and the v-fluctuation is symmetrical. On the other hand, the second harmonic component (1260 Hz) has a central peak, and two off-centre peaks, as shown in figure 10. The u-fluctuation of the component is symmetrical and the v-fluctuation is anti-symmetrical. The 0·630 Hz-component in figure 9 has a maximum value at $X = 40$ mm, whereas the maximum amplitude of 1260 Hz-component in figure 10 is found at $X = 60$ mm. Obviously, the fundamental component grows at smaller X and harmonics are amplified at larger X. The value of the 630 Hz-component is reduced considerably from $X = 40$ mm to 150 mm, while the 1260 Hz-components at those two X-stations are almost the same. Since low frequency components contribute little at $Y \neq 0$, the small values of $\overline{u^2}$ at $X = 100$ mm (figure 8) result mainly from decrease of 630 Hz-component.

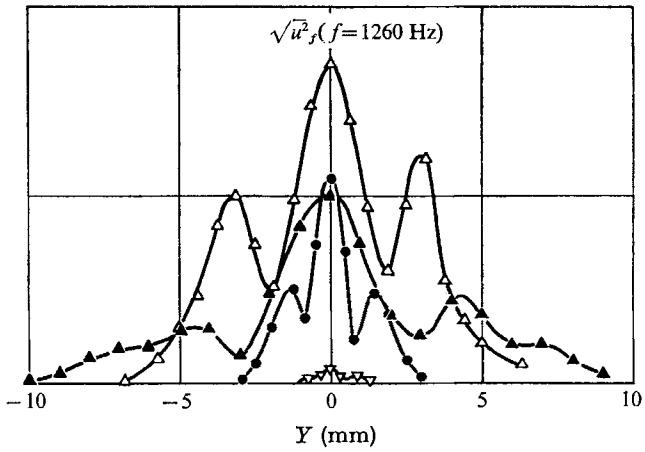

FIGURE 10. Distributions of second harmonic (1260 Hz) component. Natural transition. The ordinate scale is arbitrary. X (mm): ▽, 30; ●, 40; △, 60; ▲, 150.

4. Transition with sound of two frequencies

When a sound consisting of two different frequencies is introduced into the wake, a velocity fluctuation with two spectral components is induced. If frequencies are properly chosen, both components are amplified in the linear region. As long as their amplitudes are small, they grow independently. When amplitudes exceed certain values, a non-linear interaction takes place between the two components. Interactions occur with the mean flow as well. In the present experiment, we choose 630 Hz and 700 Hz as the frequencies of the two interacting components. Both components are amplified in the linear region with high growth rates. Intensities of the two sounds† are adjusted so that amplitudes of the two components are equal at a point in the non-linear region (about $X = 25$ mm). Since the 630 Hz-component has a higher linear growth-rate, the intensity of 700 Hz-sound was made a little higher than that of 630 Hz-sound. The process of mutual interaction depends very much on the relative magnitudes of the two components. The present experiment was made when both amplitudes were equal. We observe exactly the same amount of reduction of 700 Hz-component, when 630 Hz-sound is added to the existing 700 Hz-sound. This phenomenon was reported in Sato & Kuriki (1961) as the 'suppression effect'. The suppression is not observed in the linear region (for instance, at $X = 15$ mm).

Streamwise variations of U_c and b with various artificial disturbances are shown in figures 11 and 12. When the sound is present, the velocity on the centre-line starts increasing at smaller X and the maximum of b occurs at smaller X. However, the general trend of streamwise variations is unchanged.

Wave-forms of u-fluctuations are illustrated in figures 13 and 14 with different sweep speeds. The wave-form of sound shown at the top of each column has a

† Exactly speaking, two sinusoidal electrical signals are mixed in an amplifier before they are fed to a loudspeaker. Therefore, we have one sound with two frequencies. But for simplicity we sometimes describe as if there are two sounds.

beat with frequency of 70 Hz (= 700 Hz–630 Hz). However, this does not mean the existence of 70 Hz-sound, because two sounds are added linearly. On the other hand, the 70 Hz-component exists in the velocity fluctuation. At $X = 20$ mm, $Y = 0$, the 70 Hz-component is sinusoidal and at $X = 30$ mm, $Y = 0$ it has a flat top and a spiky bottom. This distorted wave-form indicates the presence of harmonics of the 70 Hz-component. At $Y = 2$ mm, the distortion is more pronounced. At $X = 70$ mm, $Y = 0$, the wave-form is like a saw-tooth, which contains several higher harmonics. At larger X (for example, $X = 200$ mm, $Y = 0$), the saw teeth are not regular. Irregularities seem to appear at the upper side of

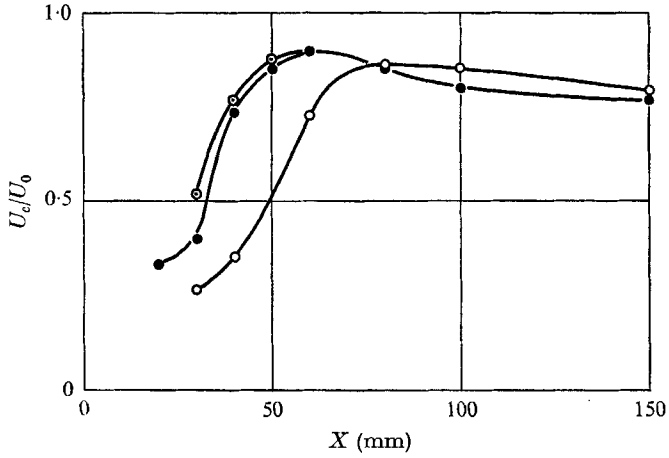

FIGURE 11. Streamwise variations of velocity on the centre-line, U_c/U_0 under various conditions: ○, no sound; ●, sound (630 Hz); ⊙, sound (630 and 700 Hz).

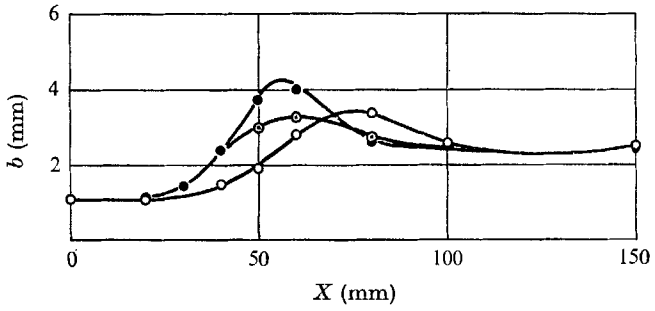

FIGURE 12. Streamwise variations of half-breadth, b under various conditions: ○, no sound; ●, sound (630 Hz); ⊙, sound (630 and 700 Hz).

the wave-form (at large u). At $X = 500$ mm, the saw-teeth have all disintegrated, and, at $X = 800$ mm, a typical turbulent fluctuation is observed. The 70 Hz-component and its harmonics might vary in X- and Y-directions in a very complicated manner, resulting in many different wave-forms. The fact that 630 and 700 Hz are multiples of 70 Hz is not essential, because similar results are obtained with different combinations of fundamental frequencies. Records with higher sweep speed (figure 14) reveal the existence of a 1330 Hz-component (sum

of 630 and 700 Hz) near the centre-line. Distorted wave-forms at various points suggest that higher harmonics are also present. The energy contained in those high-frequency components is, however, very small compared with that in low

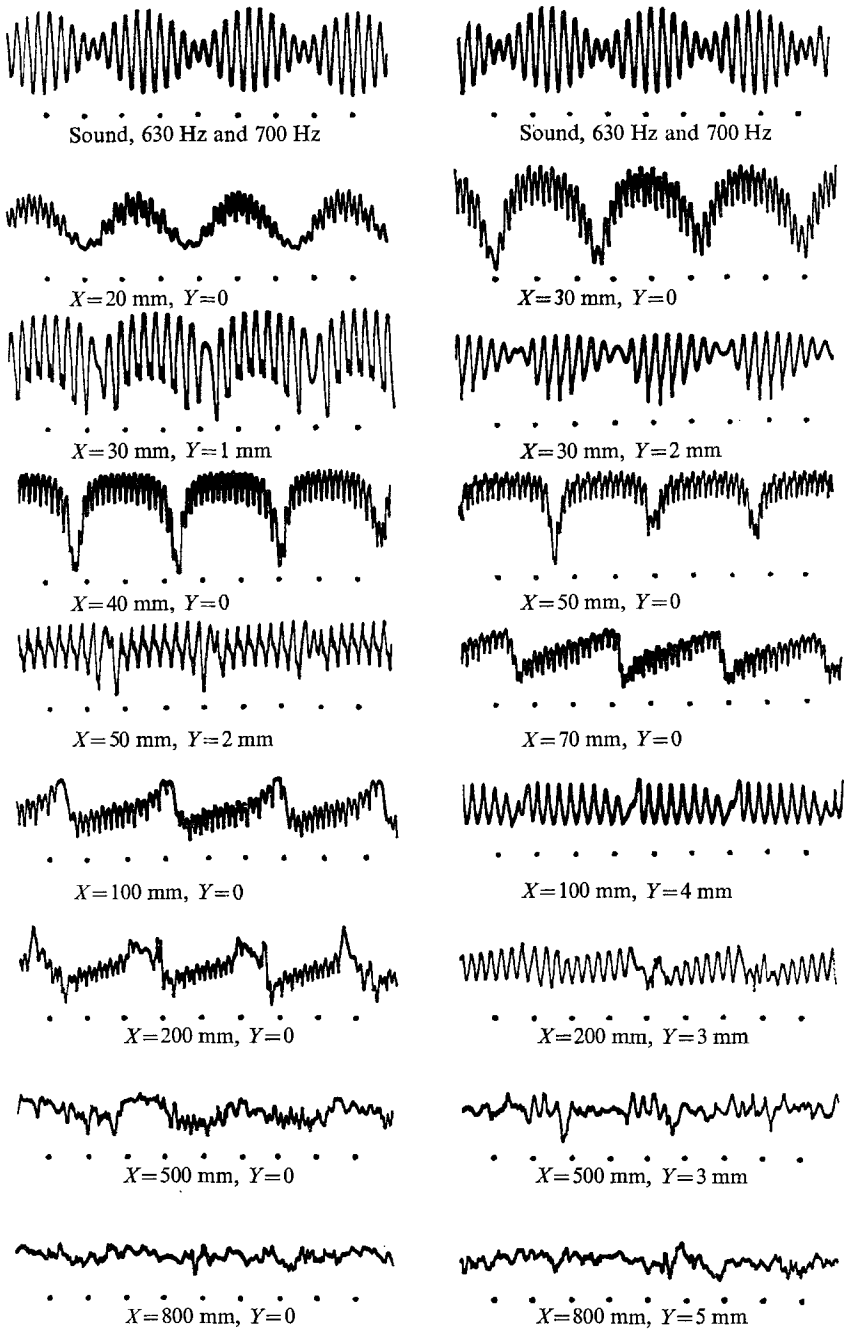

FIGURE 13. Wave-forms of u-fluctuations. Sound 630 and 700 Hz. Velocity increases upward. Time from left to right and time interval between dots is 5 msec. Uppermost traces are wave-forms of sound.

frequency components (70 Hz, 140 Hz, ...) and fundamental components (630 and 700 Hz).

Wave-forms of the v-fluctuation shown in figure 15 are considerably different. For instance, the wave-form at $X = 30$ mm, $Y = 0$ is similar to the wave-form of sound. The apparent 70 Hz-component is a linear beat. The energy of 70 Hz-

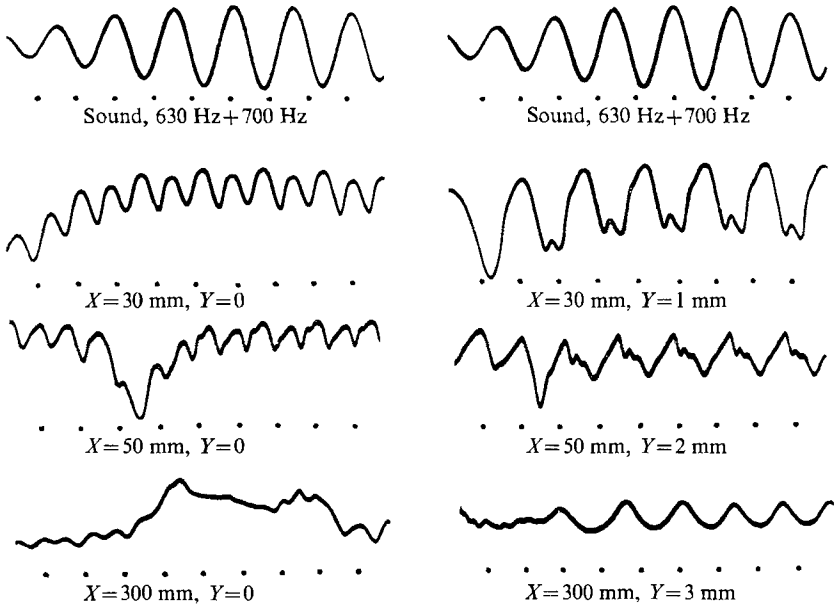

FIGURE 14. Wave-forms of u-fluctuations. Sound 630 and 700 Hz. Time interval between dots is 1 msec. Uppermost traces are wave-forms of sound.

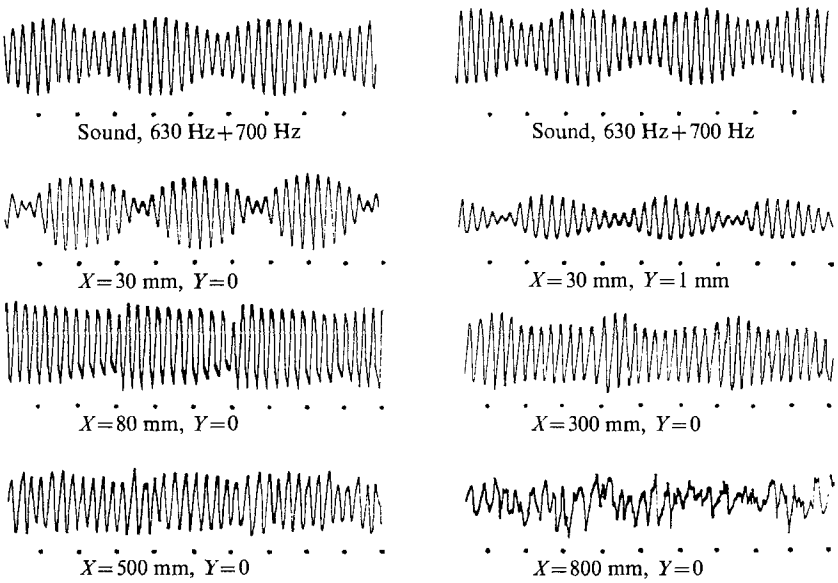

FIGURE 15. Wave-forms of v-fluctuations. Sound 630 and 700 Hz. Time interval between dots is 5 msec. Uppermost traces are wave-forms of sound.

component measured by a band-pass filter is very small throughout the whole transition region. Variations of wave-forms of the v-fluctuation in the X- and Y-directions are much simpler than those of the u-fluctuation. The wave-form is quite regular even at $X = 500$ mm and changes into turbulent pattern at $X = 800$ mm. This behaviour is similar to that of the v-fluctuation in natural transition (figure 6).

Distributions of $\overline{u^2}$, $\overline{v^2}$ and $\overline{uv}$ at two X-stations are shown in figures 16 and 17. By comparing figure 16 with figure 7 for natural transition, we find a few differences. First of all, distributions in figure 16 extend to larger Y. This is reasonable because the wake with sound is wider at $X = 40$ mm as shown in figure 12. As noticed in figures 11 and 12 the X-axis must be shifted about 20 mm to make sensible comparisons between natural and sound-induced transitions. Therefore,

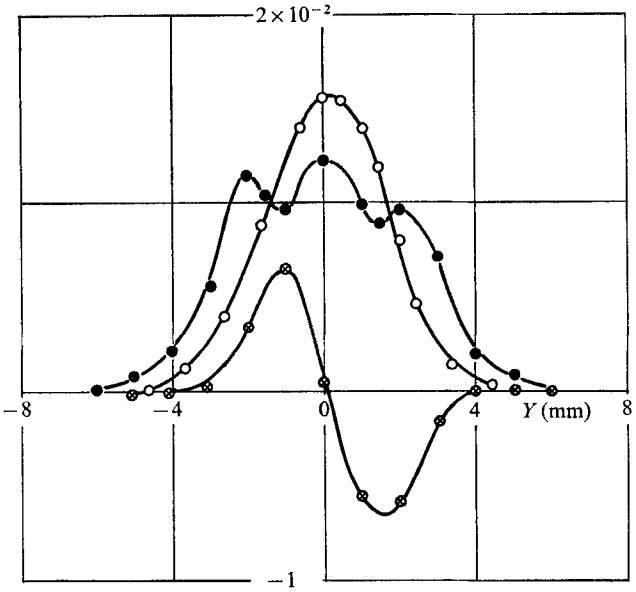

FIGURE 16. Distributions: ●, $\overline{u^2}/U_0^2$; ○, $\overline{v^2}/U_0^2$; ⊗, $\overline{uv}/U_0^2$. $X = 40$ mm. Sound 630 and 700 Hz.

detailed comparisons of absolute values in figures 16 and 7 are not meaningful. In figure 16 $\overline{u^2}$ has a peak at $Y = 0$, while in natural transition there is no such a peak. As will be shown later, amplitudes of fundamental components (630 and 700 Hz) are almost zero at $Y = 0$. Therefore, the peak is obviously due to the 70 Hz-component. Distributions of $\overline{u^2}/U_0^2$, $\overline{v^2}/U_0^2$ and $\overline{uv}/U_0^2$ at $X = 80$ mm (figure 17) are similar to those in figure 8. The sign of $\overline{uv}$ is reversed between $X = 40$ and 80 mm.

Spectra of u-fluctuations at various points in the wake are shown in figure 18. The ordinate is the amplitude of each component with an arbitrary scale. At four points on the centre-line, the 70 Hz-component and its harmonics are predominant. The 1330 Hz-component is also found. The fundamental component (630 and 700 Hz) are very small. At points off-centre ($X = 40$ mm, $Y = 2{\cdot}5$ mm

and $X = 100\,\text{mm}$, $Y = 3\,\text{mm}$), two fundamental components are predominant. The spread of each spectral component at large X is rather small. The velocity fluctuation is composed of various line spectra until $X = 500\,\text{mm}$. A continuous spectrum is formed at around $X = 800\,\text{mm}$. Spectra of the v-fluctuation consist mainly of 630 Hz-, 700 Hz- and 1330 Hz-components.

Distributions of 70 Hz-component at various X-stations are shown in figure 19. The ordinate is an arbitrary scale, while the relative magnitudes are expressed correctly. The 70 Hz-component first appears at about $X = 20\,\text{mm}$, reaches maximum between $X = 30\,\text{mm}$ and 40 mm, and then decreases. Distributions at $X = 30\,\text{mm}$ and 40 mm have a central peak and two side peaks. The central peak contributes to the value of $\overline{u^2}$ at $Y = 0$ (figure 16). The phase of the 70 Hz-component of the u-fluctuation is symmetrical with respect to the centre-line,

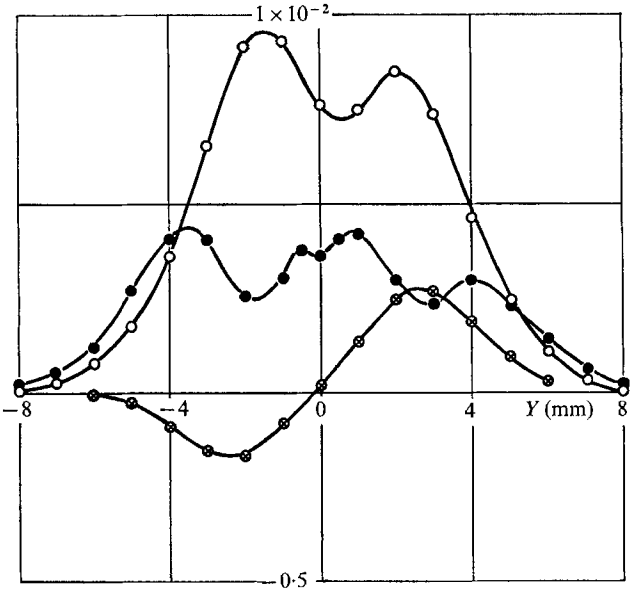

FIGURE 17. Distributions: ●, $\overline{u^2}/U_0^2$; ○, $\overline{v^2}/U_0^2$; ⊗, $\overline{uv}/U_0^2$. $X = 80$ mm. Sound 630 and 700 Hz.

and there are phase-shifts of about 180 degrees at the two off-centred dips. At $X = 80\,\text{mm}$ we find a different distribution, which is characterized by a broad central portion and small side peaks. At $X = 300\,\text{mm}$, the central peak becomes distinct again, and, at $X = 500\,\text{mm}$, the distribution is broad and flat.

Distributions of the 70 Hz-component and its harmonics are alike. They change in the stream direction also in a similar manner. At small X, the growth of each component is very rapid, but, at about 35 mm, the amplitudes reach a maximum, and then decrease down to $\frac{1}{4}$ or $\frac{1}{5}$. Since the viscous dissipation for these low-frequency components must be small, this decay may be due to some kind of energy transfer. At around $X = 60\,\text{mm}$, the amplitudes increase again with a smaller growth rate. All components repeat decay and growth once more before the turbulent wake is established at around $X = 800\,\text{mm}$.

Distributions of the 630 Hz-component at various X-stations are shown in figure 20. Distributions of 700 Hz-component are almost the same. The phase of each fluctuation is antisymmetrical with respect to the centre-line. Both fundamental components grow between $X = 20$ mm and 30 mm and then decay gradually. The three distributions at $X = 20$ mm, 30 and 40 mm are similar and resembles those in the natural transition (figure 9). At $X = 100$ mm, a different distribution is established, with two small peaks near the centre-line.

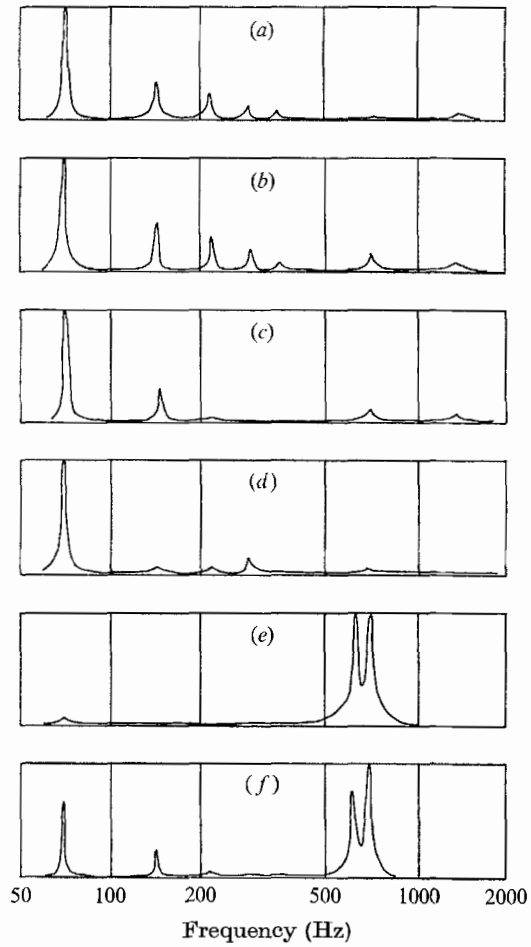

FIGURE 18. Spectra of u-fluctuations. Ordinate is root-mean-square of spectral components normalized by maximum value. Sound 630 and 700 Hz. X, Y (mm): (*a*) 40, 0; (*b*) 80, 0; (*c*) 150, 0; (*d*) 300, 0; (*e*) 40, 2·5; (*f*) 100, 3.

The phase of the 1330 Hz-component of the u-fluctuation is symmetrical with respect to the centre-line. The amplitude increases between $X = 20$ mm and 40 mm and gradually decreases downstream. The distribution at $X = 30$ mm has a central peak and two side peaks. Distributions have four side peaks at $X = 100$ mm and six side peaks at $X = 150$ mm.

In figure 21, distributions of the 70 Hz-components of $\overline{u^2}$, $\overline{v^2}$ and $\overline{uv}$ at

$X = 80$ mm are shown. The lateral component, $\overline{v_f^2}$ is very small compared with $\overline{u_f^2}$. The cross-correlation $\overline{(uv)_f}$ is also small. Measurements show that both are small at all X-stations in the transition region. In other words, the 70 Hz-component is almost a longitudinal fluctuation in X-direction. This fact is

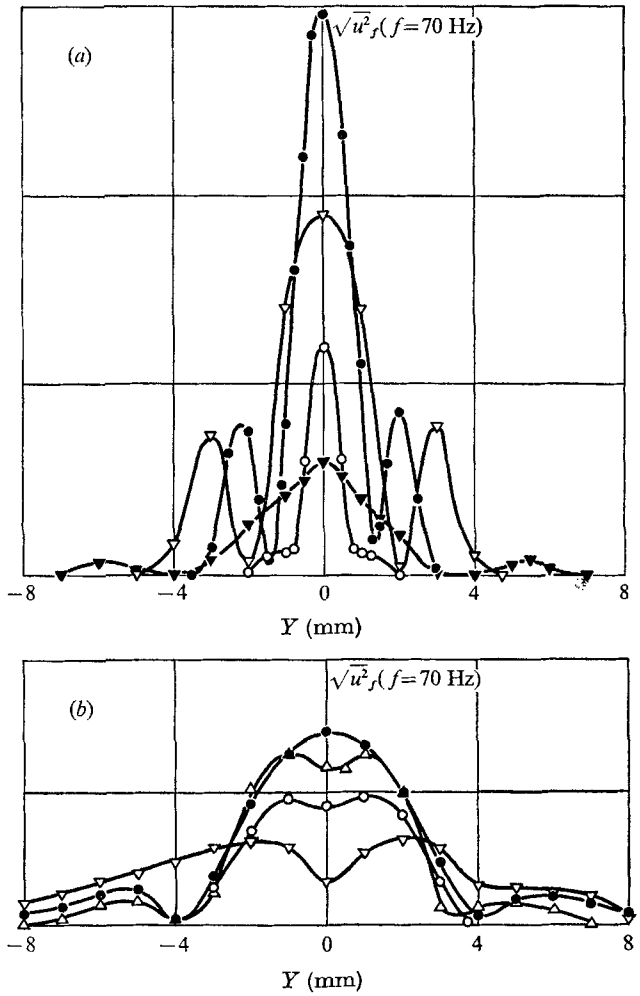

FIGURE 19. Distributions of 70 Hz-component. Sound 630 and 700 Hz. Ordinate scales are arbitrary. (*a*) X (mm): ○, 20; ●, 30; ▽, 40; ▼, 60. (*b*) X (mm): △, 80; ○, 120; ●, 300; ▽, 500.

compatible with the continuity condition. Since the wavelength of the 70 Hz-component is large, $\partial u/\partial X$ is small. This means small $\partial v/\partial Y$. Therefore, $\overline{v_f^2}$ is small. On the other hand, $\overline{v_f^2}$ of the 700 Hz-component at $X = 80$ mm, shown in figure 22, is larger than $\overline{u_f^2}$. The wavelength of the 700 Hz-component is much shorter than that of the 70 Hz-component, and therefore $\partial v/\partial Y$ is not small. The distribution of $\overline{v_f^2}$ in this figure is similar to that of $\overline{v^2}/U_0^2$ in figure 17. Distributions of $\overline{u_f^2}$ and $\overline{u^2}/U_0^2$ in the two figures show a difference, which is attributable to the contribution of the low frequency components (70 Hz, 140 Hz, ...). Values of

$\overline{u_f^2}$, $\overline{v_f^2}$ and $\overline{(uv)_f}$ are comparable for the 1330 Hz-components. Contributions of the 1330 Hz-component in the overall $\overline{u^2}$, $\overline{v^2}$ and $\overline{uv}$ are, however, very small. Thus, we can conclude that $\overline{v^2}$ and $\overline{uv}$ consist mainly of the 630 Hz- and the 700 Hz-components, while $\overline{u^2}$ is composed of two fundamental components and low-frequency fluctuations. The Reynolds stress, $-\rho\overline{uv}$, is related to the production of fluctuation energy. Fundamental components are the most significant in the production process.

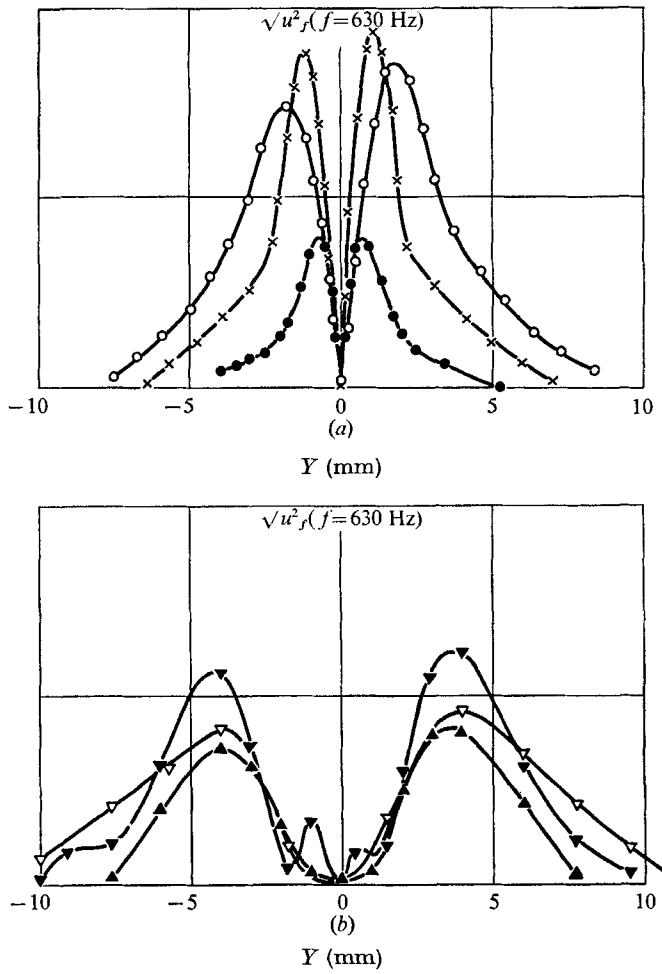

FIGURE 20. Distributions of 630 Hz-component. Sound 630 and 700 Hz. The ordinate scale is arbitrary. (*a*) X (mm): ●, 20; ×, 30; ○, 40. (*b*) X (mm): ▽, 80; ▼, 100; ▲, 150.

In Sato & Kuriki (1961), we pointed out that the fluctuation in the non-linear region is almost two-dimensional at small X and gradually becomes three-dimensional. The ratio of maximum values of $\sqrt{w^2}$ and $\sqrt{u^2}$ at each X-station is less than 0·1 at $X = 40$ mm in natural transition. It increases downstream, and reaches about 0·5 at $X = 150$ mm. In presence of two sounds, the ratio seems to reach about 0·7 at $X = 150$ mm.

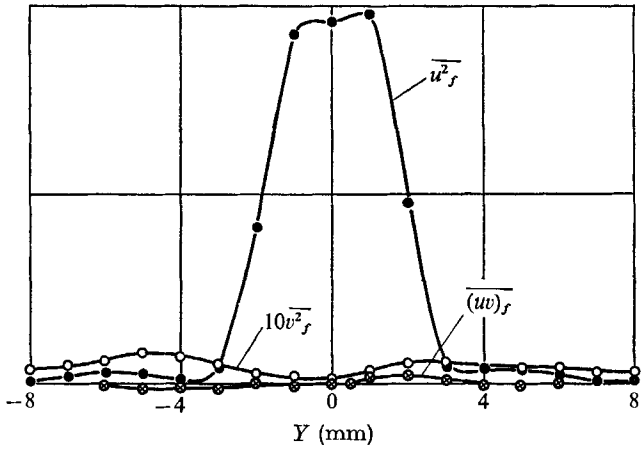

FIGURE 21. Distributions of 70 Hz-components at $X = 80$ mm: ●, $\overline{u^2_f}$; ○, $10\,\overline{v^2_f}$; ⊗, $\overline{(uv)}_f$. Sound 630 and 700 Hz. The ordinate scale is arbitrary.

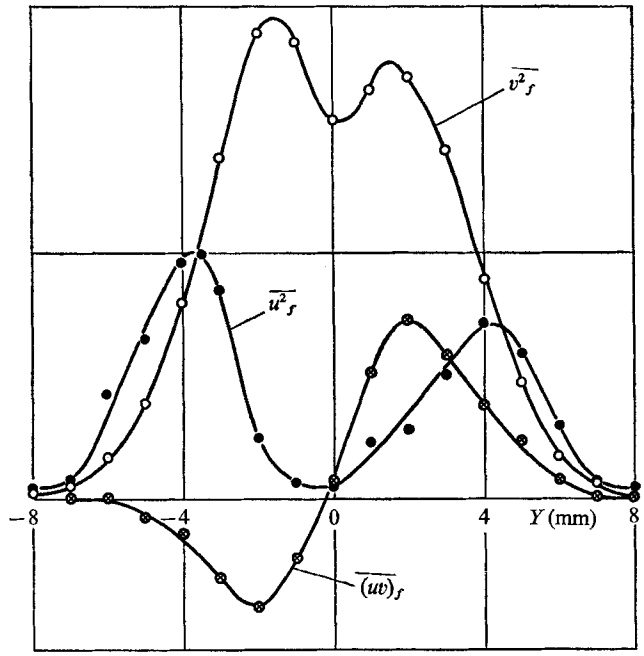

FIGURE 22. Distributions of 700 Hz-component at $X = 80$ mm: ●, $\overline{u^2_f}$; ○, $\overline{v^2_f}$; ⊗, $\overline{(uv)}_f$. Sound 630 and 700 Hz. The ordinate scale is arbitrary.

5. Discussion

The streamwise distribution of the mean velocity on the centre-line, U_c has a maximum in both natural and artificial transitions as shown in figure 11. At the same X-station the breadth of the wake b becomes a maximum and the cross correlation, $\overline{uv}$ changes the sign. A simple relation between $\overline{uv}$ and $\partial U_c/\partial X$ is

derived from the averaged Navier–Stokes equation. Neglecting viscous terms, the momentum balance on the centre-line of a two-dimensional wake is given by

$$\frac{\partial}{\partial X}\left(\frac{U_c^2}{2}+\overline{u_c^2}+\frac{P_c}{\rho}\right)+\left(\frac{\partial}{\partial Y}\overline{uv}\right)_c=0,$$

in which P is the static pressure, and subscript c denotes the value on the centre-line. Since P_c/ρ is approximated by $-\overline{v^2}$, this equation becomes

$$U_c\frac{\partial U_c}{\partial X}+\frac{\partial}{\partial X}(\overline{u^2}-\overline{v^2})_c+\left(\frac{\partial}{\partial Y}\overline{uv}\right)_c=0.$$

The second term is small compared with the first term, and U_c is always positive. Therefore, $\partial U_c/\partial X$ and $(\partial\overline{uv}/\partial Y)_c$ must have opposite signs. Since $\overline{uv}$ is zero on the centre-line, the sign of $(\partial\overline{uv}/\partial Y)_c$ determines the sign of $\overline{uv}$. Experimental results are in agreement with this simple relation.

The production of the fluctuating energy from the mean flow is given approximately by $-\overline{uv}\,\partial U/\partial Y$. Since the sign of $\partial U/\partial Y$ is the same at all X-stations, the sign of $\overline{uv}$ determines the direction of the energy transfer. At X-stations where $\partial U_c/\partial X > 0$, the energy of the mean flow is transferred to the fluctuation, and is lost by diffusion and viscous dissipation. This is the usual process to take place in most tubulent shear flows. On the other hand, in the region where $\partial U_c/\partial X < 0$, the production of the fluctuation energy is negative. In other words, the fluctuation energy is given back to the mean motion. The decrease of $\overline{u^2}$, shown in figures 8 and 17, might be due to this inverse energy transfer. Comparing figure 8 with figure 7, we observe a remarkable decrease of $\overline{u^2}$ at around $Y = \pm 2$ mm, where both $\partial U/\partial Y$ and $\overline{uv}$ are maximum. The same is true in figure 17.

For a more detailed discussion, we consider the energy balance. In a two-dimensional flow, the production and the diffusion of fluctuation energy integrated in the Y-direction at each X-station are expressed, neglecting small terms, and non-dimensional forms, by

$$-\int_{-\infty}^{\infty}\left[\frac{\overline{uv}}{U_0^2}\frac{\partial U}{\partial Y}\frac{1}{U_0}+\frac{\overline{u^2}-\overline{v^2}}{U_0^2}\frac{\partial U}{\partial X}\frac{1}{U_0}\right]dY,$$

and

$$\frac{1}{2}\frac{\partial}{\partial X}\int_{-\infty}^{\infty}\frac{\overline{u^2}+\overline{v^2}}{U_0^2}\frac{U}{U_0}dY,$$

respectively. The difference between the two is the viscous dissipation. Both terms are calculated from the experimental results with two sounds as shown in figure 23. In the figure, the production and the diffusion are almost equal. This means that the viscous dissipation is very small. In the linear stability theory of free flows, viscous terms are neglected provided the Reynolds number is large enough. Present experimental results indicate that the contribution of viscous terms is small also in the non-linear region. At $X < 60$ mm, both production and diffusion are positive. The positive diffusion means an outflow of the energy from the X-station. At $X = 40$ mm, the diffusion is larger than the production. This may be due to experimental errors. At 60 mm $< X <$ 120 mm both production and diffusion are negative. This means that the energy is supplied by the

diffusion into this region and is transferred to the mean motion. As indicated in preceding sections, the 630 Hz-component (and also the 700 Hz-component in the case with two sounds) is mainly responsible for this energy transfer.

The streamwise distribution of the static pressure on the centre-line shows a minimum near the X-station of the maximum U_c. The negative static pressure gradient ahead of the X-station may act as the accelerating force and result in the increase of U_c. At larger X, the pressure gradient is positive and the flow is decelerated, hence $\partial U_c/\partial X < 0$. Thus, distributions of U_c, $\overline{uv}$ and the static pressure are all compatible. It is difficult, however, to distinguish which one is the cause and which one is the effect.

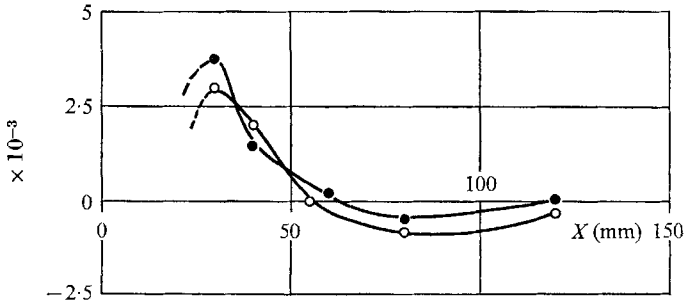

FIGURE 23. Production, ●, and convection, ○, of fluctuation energy. Sound 630 and 700 Hz.

Observations of the non-linear interaction of two spectral components in the wake indicate that one component suppresses the development of the other. For instance, the amplitude of the natural fluctuation is reduced when a sound of different frequency is introduced into the wake. Sound of higher intensity results in more reduction. Since the energy of sound itself is extremely small, this is not a direct interaction of the velocity fluctuation and the sound. The reduction is due to the interaction with the velocity fluctuation which is induced by sound and amplified in the linear region. When the frequency of sound is not in the unstable zone of the stability theory, the sound has no effect. Although the detailed mechanism is not yet clear, one possible explanation of the suppression effect is as follows. When the amplitude of the sound-induced velocity fluctuation becomes large, the mean flow interacts with the fluctuation and is distorted. The distortion may impede, or even reverse, the growth of the natural fluctuation.

When two sounds are introduced into the wake, two velocity fluctuations are induced. They grow independently in the linear region. The nature of the mutual interaction in the non-linear region depends on relative amplitudes of both fluctuations. When two amplitudes are much different, the weaker fluctuation is suppressed and the stronger fluctuation is hardly affected. On the other hand, when amplitudes of two interacting components (frequencies f_1 and f_2) are equal, we observe the same amount of suppression on each component, and the production of spectral components with frequencies, f_1-f_2, $2(f_1-f_2)$, $3(f_1-f_2)$, ... and f_1+f_2, $2(f_1+f_2)$, $3(f_1+f_2)$, ...

The frequency of the natural fluctuation in the present experiment is 630 Hz,

and the spectrum of the velocity fluctuation in the fully-developed turbulent wake extends roughly from 10 Hz to 5 KHz. In the transition process, the initial line-spectrum at 630 Hz must spread and form a broad, continuous spectrum. The high frequency side of the spectrum may be covered by the production of higher harmonics, but how are low frequency components generated? The mechanism for this must be the interaction of two spectral components, which results in the production of an $f_1 - f_2$ component. In natural transition, spectra of u-fluctuations near the centre-line have maxima between 50 and 100 Hz. Since the frequency of the fundamental component is much higher than this, we can separate the low frequency components by a high-cut filter. Distributions of $\sqrt{\overline{u^2}}/U_0$ and the low frequency components are shown in figure 24. The low frequency components are localized near the centre-line. A comparison of figures 16

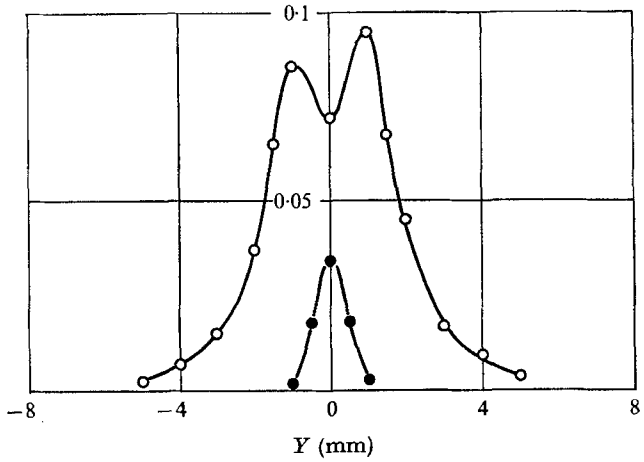

FIGURE 24. Distributions of root-mean-square of u-fluctuation, ○, and low frequency components, ●, at $X = 40$ mm in natural transition.

and 19 indicates that the 70 Hz-component is also localized near the centre-line. In the v-fluctuation in natural transition, the low frequency components are extremely small. The 70 Hz-component is also small in the v-fluctuation, as shown in figure 21. Moreover, both components grow and decay in the flow direction in a similar manner. These facts suggest that both components are produced by the same mechanism. In a wind tunnel, small disturbances with various frequencies exist. They are amplified selectively in the linear region. The non-linear interactions among amplified fluctuations will produce low frequency fluctuations. For instance, the 620 Hz-component and the 640 Hz-component have high growth rates in the linear region. They may interact with each other to produce 20 Hz-component and harmonics in the non-linear region.

This mechanism of producing slow fluctuations must be relevant to the randomization of regular fluctuations in the transition process. In nature around us nothing is strictly regular. There is a small irregularity or randomness in an apparently regular fluctuation. Although a rigorous definition of the randomness is not possible at present, we may consider the laminar-turbulent transition as a

process of amplification of a small randomness. The amplification of randomness in the natural transition may take place as follows. We consider, for instance, a 20 Hz-component produced by the interaction of 620 Hz- and 640 Hz-components. If the frequency of the first component changes by 0·1 % (from 620 Hz to 620·6 Hz) due to the inherent small randomness, the frequency of the resulting low frequency component changes to 19·4 Hz, the difference being about 3 %. The randomness is amplified 30 times. This is the basic process of the randomization in the frequency. The randomization in the amplitude might be achieved by the suppression effect. Suppose, for instance, there are two spectral components A and B in the non-linear region. Amplitudes of both components are in an equilibrium state due to the mutual suppression. A slight decrease of the amplitude of A results in a growth of B, because of less suppression by A. This, in turn, enhances the decrease of the amplitude of A due to more suppression by B. This is a feedback system which amplifies the randomness in the amplitude. The number of interacting components can be more than two. Since the turbulence field is, in general, specified in the frequency equivalent to the wave-number and amplitude space, these two processes of randomization might be sufficient for producing random, turbulent fluctuations.

Now we summarize the process of the natural transition, as follows:

An extremely small 'natural disturbance' exists in the free stream and in the laminar wake. The disturbance is irregular and composed of many spectral components. The amplitude of the disturbance is so small that the laminar wake is not affected. The disturbance is amplified in the flow direction. This amplification is selective, and a 'window' is open only for components with appropriate frequencies or wave-numbers. The selective amplification results in an almost regular velocity fluctuation in the linear region. When the amplitude of the fluctuation exceeds a certain value, non-linear interactions take place. As a result, the mean velocity distribution is deformed and the growth rate of the velocity fluctuation is reduced. At some place in the non-linear region, the amplitude of the fluctuation reaches a maximum and then decreases downstream. Most of the energy loss of the fluctuation is due to transfer back to the mean flow. The non-linear interaction also results in the generation of higher harmonics and slow irregular fluctuations. The randomization in frequency and amplitude progresses gradually and a turbulent fluctuation is formed without any abrupt breakdowns. The role of the linear region is to make a regular fluctuation from an irregular natural disturbance by selective amplification. On the contrary, the non-linear region contributes to randomization of the fluctuation.

We compare this transition process in the wake with that in the boundary layer along a flat plate. The transition in the boundary layer is characterized by a sudden breakdown and spiky bursts (Klebanoff & Tidstrom 1959; Klebanoff, Tidstrom & Sargent 1962; Tani 1969), or, in other words, by the rapid production of high frequency components. In the linear region of the boundary layer, a small amplitude disturbance is amplified in a similar way as in the wake. However, there are significant quantitative differences. One is the frequency (wavelength), and the other is the growth rate of the fluctuation. In the wake, according to the linear theory, the fluctuation with the maximum growth rate has a wavelength

of about 4δ, δ being twice the half-breadth b. If the streamwise amplification is expressed by $e^{\mu x}$, the maximum value of μ for the wake is about $0{\cdot}4/\delta$. On the other hand, in the boundary layer with Reynolds number $U_0\delta^*/\nu$ about 10^4, the fluctuation with maximum growth rate has a wavelength of 30δ, and a maximum μ on the order of $0{\cdot}01/\delta$. Therefore, in the wake a fluctuation with a short wavelength grows very rapidly, whereas in the boundary layer a fluctuation with long wavelength is amplified gradually. In other words, in the linear region, the time scale in the wake is much shorter than that in the boundary layer. Since time-scales of fluctuations in a fully-developed, turbulent wake and boundary layer are not much different, the linear growth in the wake must be followed by a relatively 'slow' process. Contrariwise, some 'fast' change is necessary in the boundary layer. Thus, the production of slow fluctuations in the wake and the sudden breakdowns in the boundary layer are both essential. The linear region is not a simple 'pre-amplifier' in the transition process, but it has a decisive effect in the later development of fluctuations. The nature in the transition processes in various flow field should be clarified in connexion with the characteristics of the linear regions.

6. Conclusion

Experimental results on the transition process of a two-dimensional wake indicate the following conclusions.

(i) In natural transition, a regular velocity fluctuation is observed as a result of a selective amplification of irregular natural disturbances. As the fluctuation grows, higher harmonics, and a slow, irregular fluctuation are generated. The transition process is gradual, and there are no abrupt breakdowns.

(ii) When a sound is introduced into the wake, a small-amplitude velocity fluctuation is induced. With a sound composed of two frequencies f_1 and f_2, two velocity fluctuations are induced. If frequencies are properly chosen, both fluctuations are amplified in the linear region. Due to the non-linear interaction, velocity fluctuations with frequencies of f_1-f_2, $2(f_1-f_2)$, $3(f_1-f_2)$, ... and f_1+f_2, $2(f_1+f_2)$, $3(f_1+f_2)$, ... are produced.

(iii) In both cases, with and without sound, the streamwise distribution of the mean velocity on the centre-line has a maximum. In other words, there is a region in which the central velocity decreases in flow direction. In this region, the sign of Reynolds stress is such that the energy is transferred from the fluctuation into the mean flow.

(iv) The behaviour of the slow, irregular fluctuation in natural transition resembles that of the f_1-f_2 component in the sound-induced transition. The slow fluctuation seems to be produced by the non-linear interaction between amplified natural fluctuations.

(v) The concept of 'amplification of randomness' is useful in considering the change of a regular fluctuation into random turbulence. A small randomness in the frequency is amplified when two spectral components interact and produce a low frequency component. The randomization of the amplitude is accomplished by the mutual suppression of spectral components.

(vi) The difference in the transition processes of the boundary layer and of the wake is partly due to the difference in the nature of the linear region. In the boundary layer, a low frequency fluctuation is amplified gradually in the linear region and fast breakdowns follow. In the wake, a high frequency fluctuation grows rapidly and slow fluctuations are generated in the non-linear region.

The author is grateful to Mr Yoshio Onda, who helped to carry out the experimental program.

REFERENCES

BENNEY, D. J. 1961 *J. Fluid Mech.* **10**, 209–236.

BROWAND, F. K. 1966 *J. Fluid Mech.* **26**, 281–307.

KELLY, R. E. 1968 *J. Fluid Mech.* **31**, 789–799.

KLEBANOFF, P. S. & TIDSTROM, K. D. 1959 *NASA T.N.* D-195.

KLEBANOFF, P. S., TIDSTROM, K. D. & SARGENT, L. M. 1962 *J. Fluid Mech.* **12**, 1–34.

SATO, H. 1959 *J. Phys. Soc. Japan*, **14**, 1797–1810.

SATO, H. & KURIKI, K. 1961 *J. Fluid Mech.* **11**, 321–352.

SATO, H. & ONDA, Y. 1970 *Report Inst. Space & Aero. Sci. University of Tokyo.* (To be published.)

TANI, I. 1969 *Annual Review of Fluid Mechanics*, **1**, 169–196.